Arteriovenous shunting is not associated with venous congestion in bone

Knee tamponade studied with 15-μm and 50-μm microspheres in immature dogs

Ebbe Stender Hansen[1, 2, 3], Vibeke Elisabeth Hjortdal[2], Dorthe Kjølseth[2], Shu-Zheng He[1], Kristian Høy[1], Kjeld Søballe[1, 2] and Cody Bünger[1]

Blood flow in the hind-limb bones of 8 immature labrador dogs with unilateral knee joint tamponade at 75 percent of the mean arterial pressure was measured with 15-μm and 50-μm microspheres to determine whether or not arteriovenous shunting occurs in bone with venous congestion caused by increased outflow resistance. The intraosseous pressure was 43 percent of the mean arterial pressure in the experimental distal femoral epiphysis versus 14 percent in the control knee ($P < 0.001$). No pressure changes were found in the distal femoral metaphysis. Regional blood flow with 15-μm microspheres decreased centrally in the distal femoral epiphysis and increased centrally in the proximal tibial epiphysis. Metaphyseal blood flow was largely unchanged. A net shift in the preferred embolization site of 50-μm microspheres relative to that of 15-μm microspheres from central to peripheral regions occurred within both juxta-articular epiphyses, indicating arteriolar vaso-dilation, but the relation between the uptake of the two microsphere sizes was unchanged when the epiphyses and other bony flow compartments were viewed in toto. The result speaks against the hypothesis of arteriovenous shunting in intra-osseous hypertension.

[1]Orthopedic Hospital, [2]Institute of Experimental Clinical Research, and [3]Department of Clinical Physiology and Nuclear Medicine, University of Århus, Denmark
Correspondence: Dr. Ebbe Stender Hansen, Orthopedic Hospital, Randersvej 1, DK-8200 Århus N, Denmark
Submitted 90-05-16. Accepted 90-12-28

Increased intraosseous pressure (IOP) is a painful adjunct of inflammatory and degenerative diseases of joints (Arnoldi et al. 1975, Arnoldi and Reimann 1979, Arnoldi et al. 1980). The mechanism involves impairment of the venous drainage from bone due to intraosseous vascular pathology (He et al. 1990) or extraosseous venous compression secondary to interstitial edema or joint effusion (Bünger 1987). An intimate association exists between intraarticular pressure (IAP) and IOP in the epiphyses and patella during tamponade of the immature dog knee (Bünger 1987), apparently accompanied by auto-regulation of arteriolar tone to maintain epiphyseal blood flow in the face of venous outflow obstruction (Bünger 1987, Ewald et al. 1989, Holm et al. 1989). Both precapillary vasodilation and postcapillary stasis could cause opening of intraosseous arterio-venous (AV) communications, and thus contribute to the elevated IOP and amplification of the pulse amplitude within bone following knee joint tamponade.

We performed bone blood flow analysis with the combination of 15-μm and 50-μm microspheres (MSs; Guba 1980) in young dogs with artificially elevated IAP of one knee to test the hypothesis that the ensuing elevated IOP is associated with enhanced AV shunting in bone. The hypothesis is presented schematically in Figure 1.

Material and methods

Animals

Eight immature labrador dogs, 6–7 months of age, weighing 15.5–25.0 kg were used. The dogs were bred for scientific purposes and handled according to the Danish law on animal experimentation.

Preparation

The dogs were premedicated with Combelen vet.® (propionyl promazine). Anesthesia was induced with i.v. methohexital sodium (Brietal®, 7 mg/kg) and maintained with intermittent doses of Immobilon® (etorphine 0.125 mg + acepromazine

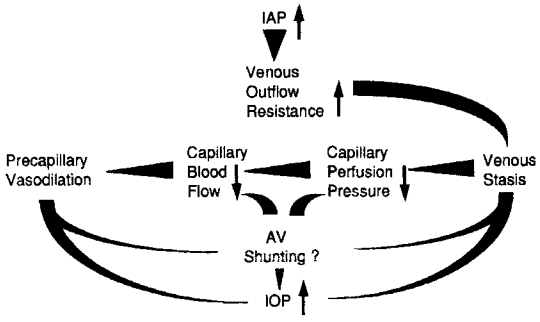

Figure 1. Schematic presentation of the hypothesis tested in this experiment: Increased intraarticular pressure (IAP) causes increased venous outflow resistance from juxtaarticular bone, resulting in intraosseous venous stasis, decreased capillary perfusion pressure, and decreased capillary blood flow. Reduced bone blood flow in turn elicits autoregulatory arteriolar dilation to maintain capillary perfusion. Venous stasis and precapillary vasodilation both contribute to the increased intraosseous pressure (IOP) measured by bone cannulation. Our hypothesis was that arteriolar dilation and venous stasis both could cause opening of arteriovenous (AV) shunts in bone. AV shunting then would influence the capillary perfusion adversely by reduction of the capillary perfusion pressure and redirection of a volume of blood away from the capillary bed. In addition, AV shunting could cause arterialization of venous blood in bone and thus contribute directly to elevation of the intraosseous pressure.

0.4 mg per mL) and Pavulon® (pancuronium bromide). After orotracheal intubation, the dogs were positioned supine and ventilated mechanically on a constant volume respirator. The lower limbs were supported in slight abduction and neutral rotation with the knees at the same horizontal level in unrestrained semiflexion. The carotid arteries were exposed through a midline incision, and a pigtail catheter was inserted into the left ventricle through the left carotid artery. A straight end catheter with multiple side perforations was directed into the aorta through the right carotid artery and advanced to the level of the 4th lumbar vertebra. Catheters were inserted into the left brachial artery and both femoral veins through small skin incisions. The distal femoral epiphyses and metaphyses were cannulated bilaterally by percutaneous insertion of Radner bone cannulae (Bünger 1987), perfused at a rate of 0.5 mL/h by a Braun-Melsungen heavy duty infusion pump. IOP in the four bone locations and mean arterial pressure (MAP) were monitored continuously using a fluid filled electromanometric system consisting of Statham transducers and amplifiers connected to a Mingograph 81. The dogs were heparinized at the time of bone cannulation (400 IU/kg) to avoid clotting of catheters and cannulae. Arterial gases were analyzed repeatedly (ABL1, Radiometer).

Experimental procedure

IAP was raised in the right knee to 75 percent of MAP after 30 min of cardiopulmonary steady state by elevating a bottle of dextran 60 (Macrodex) connected via a three-way stop cock to an injection cannula positioned obliquely through the inferior patellar ligament with the tip in the intercondylar compartment. Blood flow was measured after 2 h of steady joint tamponade: Two vials of NEN-TRAC microspheres, suspended in dextran 70 with 0.01 percent Tween 80, were agitated simultaneously for 30 min on a Whirlimixer. One vial contained 6 MBq ^{141}Ce-labeled 15-μm MSs (12×10^6 particles, specified diameter 16.5 ± 0.1 μm), the other contained 4 MBq ^{46}Sc-labeled 50-μm MSs (0.6×10^6 particles, specified diameter 48.4 ± 0.2 μm). MSs were injected, 15-μm MSs first, over 30 sec per vial into the intraventricular catheter. Reference blood was withdrawn for 4 min, beginning 30 sec before MS injection, from the left brachial artery (rate 5 mL/min), the abdominal aorta (rate 10 mL/min), and both femoral veins (rate 5 mL/min) with siliconated glass syringes driven by a reversed Braun-Melsungen infusion pump. The femoral vessels were clamped simultaneously, and the dogs were killed with intracardiac potassium chloride. Dissection was performed immediately.

Counting procedure and calculations

The total activity in each MS vial was determined in an Amersham Radioisotope Calibrator (ARC 120, Capintec Inc. NJ, U.S.A.) before injection. After the experiment, all the remnants were measured and subtracted to obtain the injected dose in MBq. A predetermined MBq quantity of each MS type was suspended in tap water and vortexed, and twenty 1-mL aliquots were withdrawn for determination of counting efficiency (cpm/MBq) of the gamma counter for the isotopes used. Standards and tubes were counted by multichannel gamma spectrometry (Packard COBRA) with automatic background subtraction. All the counts were corrected for cross talk between isotopes and adjusted to a common reference time by use of appropriate decay equations. (Two other isotopes, irrelevant to the subject of this paper, were used, and the spectrometric cross-talk correction was based on counting in the following windows: 15–75 KeV (^{125}I), 115–180 KeV (^{141}Ce), 240–400 KeV (^{51}Cr), and 800–940 (^{46}Sc)). Cardiac output (CO) was calculated from MS injectates (MS_{inj}) and total MS count in the reference blood (MS_{ref}) using the

Table 1. Cardiac output (L × min^{-1}) determined by 15-μm and 50-μm microspheres (MSs) sampled simultaneously from the brachial artery and aorta during intracardiac injection

	15-μm MSs	50-μm MSs	50-μm MSs/ 15-μm MSs
B	1.77 (0.17)	2.66 (0.34)[a,b]	1.53 (0.17)
A	1.65 (0.14)	2.14 (0.24)[a]	1.31 (0.08)
B/A	1.10 (0.09)	1.23 (0.06)	–

B Brachial artery, A aorta.
[a] $P < 0.01$, 50-μm MS value compared with 15-μm MS value.
[b] $P < 0.01$, brachial arterial value compared with the aortic value.

equation $CO = MS_{inj} \times$ sampling rate/MS_{ref}. The fraction of the microsphere injection taken up by a biopsy (the fractional uptake, F) was calculated from the biopsy count of each MS type (MS_{biop}) by the ratio $F = MS_{biop}/MS_{inj}$. The regional blood flow was then calculated for the 15-μm MSs (RBF_{15}) and the 50-μm MSs (RBF_{50}) by multiplication of CO with F for the two MS types, and was expressed as standardized flow in mL × min^{-1} × 100g^{-1}. The relative distribution of 50-μm MSs and 15-μm MSs was expressed as the ratio between RBF_{50} and RBF_{15}. The fraction of MSs escaping entrapment in the lower limbs during injection was calculated as venous MS count/venous sampling rate divided by arterial MS count/arterial sampling rate and expressed as a nonentrapment percentage. By counting a central venous blood sample drawn after microsphere injection we found no circulating ^{141}Ce or ^{46}Sc activity, indicating that the microspheres did not leach radioactivity.

Statistic parameters were ln-transformed to stabilize variances and tested statistically with ANOVA and the Student's paired *t*-test. The risk of mass significance in multiple simultaneous comparisons was assessed by the sum $2 \times \sum_1^n \ln(p_i)$ of n independent p values, which under the null hypothesis of no significant differences will be chi-square distributed with 2n degrees of freedom (Fisher 1932). Untransformed values (mean, SEM) were used for tabulation.

Results

Central hemodynamics

The MAP (mean, SEM) was 112 (8) mmHg and the heart rate 78 (6) min^{-1} at the time of blood flow measurement. CO values differed according to reference sampling site and MS size (Table 1). Greater values were obtained with the large MS, which suggests relative underrepresentation of these spheres in arterial reference blood. The brachial artery sampling yielded greater values than the aortic sampling when calculated on the basis of the large MS, but not the small MS, indicating relatively greater underrepresentation of 50-μm MSs in the brachial artery reference sample. The CO value reached with 15-μm MSs and aorta sampling was used in all the additional calculations.

Intraosseous pressure (Table 2)

IOP at the time of blood-flow measurement was elevated in the distal femoral epiphysis, but not in the metaphysis.

Table 2. Mean arterial pressure (MAP, mmHg) and intraosseous pressure (mmHg, percent of MAP in parentheses) in the distal femoral epiphysis and the distal femoral metaphysis following unilateral knee joint tamponade at 75 percent of MAP

		Experimental		Control	
Dog	MAP	Epiphysis	Metaphysis	Epiphysis	Metaphysis
1	90	45 (50)	20 (22)	13 (14)	14 (16)
2	91	47 (52)	17 (19)	19 (21)	22 (24)
3	85	55 (65)	15 (18)	13 (15)	26 (31)
4	100	36 (36)	26 (26)	10 (10)	9 (9)
5	145	67 (46)	28 (19)	21 (14)	25 (17)
6	145	40 (33)	10 (7)	13 (9)	18 (12)
7	120	39 (33)	17 (14)	12 (10)	14 (12)
8	120	43 (36)	8 (7)	20 (17)	9 (8)
Mean	112	47 (43)[a,b]	18 (16)	15 (14)	17 (16)

[a] $P < 0.001$, compared with the ipsilateral metaphysis.
[b] $P < 0.001$, compared with the control epiphysis.

Table 3. Nonentrapment (percentage) of 15-μm and 50-μm microspheres (MSs) in the lower limbs of dogs with unilateral knee joint tamponade at 75 percent of mean arterial pressure

	15-μm MSs		50-μm MSs	
Dog	Experimental	Control	Experimental	Control
1	5.8	2.7	0.0	0.0
2	10.9	15.7	1.1	0.4
3	10.0	20.2	1.0	0.0
4	11.6	6.9	2.1	0.0
5	8.3	7.4	0.4	0.5
6	61.8	21.4	26.0	11.2
7	13.9	15.3	0.3	0.1
8	7.5	5.1	0.7	0.5
Mean	16.2[a]	11.8[a]	3.9[b]	1.6

[a] $P < 0.01$, compared with the ipsilateral 50-μm MS value.
[b] $P < 0.02$, compared with the control limb value.

Nonentrapment of microspheres (Table 3)

The interindividual variability in overall nonentrapment of MSs in the lower limbs was considerable. Significantly more 15-μm MSs than 50-μm MSs escaped entrapment in both lower limbs. Nonentrapment of 15-μm MSs did not differ significantly between experimental and control limbs, but nonentrapment of 50-μm MSs was significantly enhanced in experimental limbs.

Blood flow

Results of the blood-flow analysis with the two different MS sizes are summarized in Tables 4–6.

RBF_{15} exhibited a characteristic pattern of distribution in both femur and tibia with lower central and higher peripheral epiphyseal values and U-shaped metaphyseal profiles with high values in growth plates and in bone bordering on the medullary cavity and very low values in the spongiosa immediately behind the zones of growth. Knee-joint tamponade caused the central epiphyseal RBF_{15} to decline in the distal femoral epiphysis and to rise in the proximal tibial epiphysis, whereas significant changes were not observed in the juxtaarticular metaphyses or in more remote bone locations relative to the knee joint.

The RBF_{50} distribution generally reproduced that of RBF_{15} with the following three exceptions: First, RBF_{50} was significantly lower than RBF_{15} in both femora and tibiae viewed in toto, due to a lower uptake of the larger MSs in the diaphyseal cortex and the epiphyses. Secondly, no RBF_{50} gradients existed between the central and peripheral epiphyseal bone. Thirdly, the metaphyseal gradients were less steep with higher RBF_{50} than RBF_{15} values in the metaphyseal bone adjacent to growth plates.

Changes in RBF_{50} during knee-joint tamponade generally followed the same trends as RBF_{15}. The ratio between RBF_{50} and F_{15} remained unaffected by joint tamponade when larger bone aggregates or whole flow compartments—such as the juxtaarticular epiphyses, shafts, and the entire long bones—were viewed in toto. However, the ratio between RBF_{50} and RBF_{15} tended to go down in central and up in peripheral epiphyseal locations in experimental knees, indicating a net downstream shift in embolization site of 50-μm MSs from central to peripheral locations. By intraindividual analysis, this shift was significant in both the distal femoral epiphysis (Table 5) and the proximal tibial epiphysis (Table 6). Joint tamponade appeared to facilitate entry of 50-μm MSs into the diaphyseal cortex of femur.

Table 4. Regional blood flow (mL x min^{-1} x $100g^{-1}$) in patella and soft tissues around the knee determined with 15-μm and 50-μm microspheres (RBF_{15} and RBF_{50}, respectively) during unilateral joint tamponade at 75 percent of the mean arterial pressure. Mean *SEM*, n 8

	RBF_{15}				RBF_{50}				RBF_{50}/RBF_{15}	
	E		C		E		C		E/C	
Skin over patella	2.2	*0.4*	2.3	*0.4*	0.6	*0.2*[d]	0.9	*0.3*[c]	1.02	*0.39*
M. tibialis anterior	6.4	*1.8*	6.9	*1.0*	5.5	*0.9*[b]	7.7	*1.1*	0.90	*0.09*
M. vastus lateralis	4.8	*1.4*	4.6	*0.9*	5.2	*1.0*	4.7	*1.0*	1.49	*0.44*
Joint capsule	2.6	*0.6*[a]	1.1	*0.3*	2.1	*0.6*[a]	1.0	*0.2*	0.62	*0.08*[e]
Synovial membrane	2.8	*0.7*	2.1	*0.6*	1.7	*0.3*[c]	2.6	*0.8*	1.42	*0.51*
Patella	4.0	*0.8*	5.4	*1.1*	2.5	*0.9*[c]	1.8	*0.7*[d]	5.91	*3.84*

E Experimental knee, C control knee.
[a] $P < 0.05$, [b] $P < 0.01$; experimental knee value compared with control knee value.
[c] $P < 0.05$, [d] $P < 0.01$; RBF_{50} compared with RBF_{15} in the same location.
[e] $P < 0.05$; different from expected 1.00.

Table 5. Regional blood flow (mL × min^{-1} × 100g^{-1}) in femur determined with 15-μm and 50-μm microspheres (RBF_{15} and RBF_{50}, respectively) during unilateral joint tamponade at 75 percent of the mean arterial pressure. Mean *SEM*, n 8

	RBF_{15}				RBF_{50}				RBF_{50}/RBF_{15}	
	E		C		E		C		E/C	
FEMUR, total	9.4	*1.1*	9.9	*1.3*	7.3	*1.0***	7.9	*1.4***	1.00	*0.03*
Periosteum	8.1	*0.9*	8.2	*1.3*	7.9	*2.0*	8.1	*1.1*	1.20	*0.15*
Head	6.5	*0.8*	6.0	*0.9*	5.2	*1.1**	5.5	*1.0*	0.92	*0.17*
Shaft[a]	10.7	*1.3*	10.8	*1.3*	8.4	*1.2**	8.8	*1.4**	0.99	*0.04*
Central shaft[b]	14.6	*1.9*	15.0	*1.8*	12.8	*1.9*	13.6	*2.4*	0.99	*0.04*
Cortex, total	6.2	*0.8*	6.0	*0.9*	3.5	*0.5****	3.2	*0.5****	1.06	*0.05*
Proximal metaphysis	13.2	*1.7*	14.1	*1.9*	10.8	*1.5*	12.3	*1.9*	0.96	*0.05*
Diaphysis	7.5	*0.9*	7.3	*0.8*	3.8	*0.9***	3.5	*1.0***	1.18	*0.12*
Cortex	4.9	*0.6*	4.4	*0.5*	1.1	*0.2****	0.6	*0.2****	2.40	*0.71*[c]
Marrow	15.0	*2.3*	14.9	*1.9*	12.0	*3.2*	11.4	*3.7**	1.16	*0.10*
Distal metaphysis	12.1	*1.9*	11.9	*1.7*	11.7	*2.1*	11.6	*1.8*	0.99	*0.05*
Cortex	7.7	*1.1*	7.9	*1.2*	7.0	*1.3*	7.3	*0.9*	0.96	*0.10*
Spongiosa	14.8	*2.5*	14.5	*2.3*	14.7	*2.8*	14.6	*2.7*	1.02	*0.07*
Proximal	19.9	*2.9*	19.3	*1.9*	21.7	*4.9*	18.7	*3.2*	1.10	*0.12*
Intermediary	8.6	*2.0*	9.4	*2.2*	9.8	*2.3*	9.4	*2.3*	1.35	*0.25*
Distal	1.8	*0.4*	2.7	*0.6*	3.8	*0.6***	7.0	*1.8***	0.95	*0.11*
Growth plate	31.3	*6.6*	31.1	*7.2*	25.1	*7.5***	25.9	*6.7*	1.02	*0.10*
Distal epiphysis	6.3	*0.5*	8.4	*1.3*	3.6	*0.6***	4.8	*1.3***	1.12	*0.17*
Center	4.0	*0.3*#	5.4	*0.6*	3.4	*0.6*	5.7	*1.0*	0.89	*0.14*[d]
Periphery	7.6	*0.6*	10.0	*1.8*	3.6	*0.7***	4.4	*1.4****	1.32	*0.21*

E Experimental knee, C control knee.
#$P < 0.05$; experimental knee value compared with control knee value.
*$P < 0.05$, **$P < 0.01$, ***$P < 0.001$; RBF_{50} compared with RBF_{15} in the same location.
[a]Shaft defined as total femur minus the femoral head and minus the distal femoral epiphysis.
[b]Central shaft defined as shaft minus total cortex.
[c]$P < 0.05$; different from 1.00.
[d]$P < 0.001$; center vs periphery.

Table 6. Regional blood flow in tibia determined with 15-μm and 50-μm microspheres (RBF_{15} and RBF_{50}, respectively) during unilateral joint tamponade at 75 percent of the mean arterial pressure. Mean *SEM*, n 8

	RBF_{15}				RBF_{50}				RBF_{50}/RBF_{15}	
	E		C		E		C		E/C	
TIBIA, total	7.3	*1.0*	7.2	*1.1*	5.8	*1.0****	5.4	*1.0****	1.07	*0.05*
Periosteum	4.7	*0.9*	5.4	*0.7*	4.9	*1.3*	5.4	*1.0*	1.63	*0.31*
Proximal epiphysis	8.0	*1.0*	7.3	*1.4*	3.8	*1.0****	3.4	*1.2***	1.24	*0.15*
Center	5.6	*0.8*#	4.5	*1.0*	3.1	*0.9**	3.3	*1.1**	0.83	*0.15*[d]
Periphery	9.6	*1.3*	9.1	*2.0*	4.2	*1.2****	3.4	*1.3****	1.86	*0.34*[c]
Shaft[a]	7.8	*1.1*	7.6	*1.3*	6.5	*1.1***	6.1	*1.2****	1.06	*0.06*
Central shaft[b]	13.6	*1.9*	13.9	*2.1*	13.3	*2.1*	13.0	*2.4*	1.07	*0.06*
Cortex, total	3.9	*0.6*	3.8	*0.7*	2.1	*0.4****	1.9	*0.3****	1.09	*0.13*
Proximal metaphysis	11.6	*1.7*	10.9	*2.0*	9.7	*1.9**	8.4	*0.7****	1.14	*0.10*
Cortex	6.1	*0.9*	5.8	*1.1*	4.0	*0.9***	3.8	*0.7****	0.95	*0.09*
Spongiosa	16.7	*2.6*	16.2	*2.7*	15.2	*2.9*	13.0	*2.8***	1.25	*0.17*
Growth plate	31.0	*5.5*	30.7	*5.0*	29.8	*6.6*	26.3	*6.1**	1.25	*0.19*
Proximal	5.9	*1.4*	5.0	*1.4*	6.2	*1.0*	4.5	*1.3*	2.22	*0.83*
Intermediary	17.0	*2.2*	15.5	*2.9*	11.3	*3.1**	9.9	*1.9****	0.87	*0.12*
Distal	15.8	*2.0*	13.9	*2.5*	11.2	*1.9**	9.0	*2.3**	1.68	*0.39*
Diaphysis	3.2	*0.5*	3.2	*0.5*	1.2	*0.2****	1.4	*0.4****	0.99	*0.08*
Cortex	2.4	*0.4*	2.4	*0.4*	0.4	*0.1****	0.5	*0.2****	1.43	*0.44*
Marrow	6.6	*1.1*	6.7	*1.1*	5.1	*0.9**	5.9	*1.4*	1.12	*0.28*
Distal metaphysis	9.6	*1.6*	10.9	*1.9*	11.2	*1.9*	12.0	*1.9*	1.04	*0.10*
Distal epiphysis	4.1	*0.8*	3.9	*0.5*	1.2	*0.6**	0.7	*0.2***	2.20	*0.82*

E Experimental knee, C control knee.
#$P < 0.05$; experimental knee value compared with the control knee value.
*$P < 0.05$, **$P < 0.01$, ***$P < 0.001$; RBF_{50} compared with RBF_{15} in the same location.
[a]Shaft defined as total femur minus the femoral head and minus the distal femoral epiphysis.
[b]Central shaft defined as shaft minus total cortex.
[c]$P < 0.05$; different from 1.00.
[d]$P < 0.05$; center vs periphery.

The formal statistical probability that the changes in RBF_{15} and RBF_{50} in experimental limbs reported merely expressed mass significance exceeded 5 percent. However, these changes exclusively occurred in structures directly affected by the joint tamponade (juxtaarticular epiphyses, joint capsule, distal femoral metaphysis), which justifies the interpretation of the findings as real physiologic trends. Differences between RBF_{50} and RBF_{15} could not be ascribed to mass significance.

Discussion

Enhanced AV shunting in experimental knees would have caused elevation of the ratio between RBF_{50} and RBF_{15} due to selective nonentrapment of 15-μm MSs. This ratio was unchanged in all larger bony aggregates or flow compartments, including the juxtaarticular epiphyses, indicating that such shunt opening did not occur in bone. Because the pressure level used was selected as that producing the greatest IOP response (Bünger 1987), it appears that AV shunting plays no role in intraosseous venous engorgement. A comparable result was reached in a similar study of AV shunting in juvenile gonarthritis (Hansen et al. 1990b). The validity of this negative statement may be assessed by construction of the 95 percent confidence intervals for the experimental to control ratio of the RBF_{50}/RBF_{15} ratios. In femur this ratio was 1.00, with the confidence interval 0.94–1.07, indicating that the difference in nonentrapment of 15-μm MSs between the experimental and the control femur should exceed 7 percent to be detected in this experiment. In the distal femoral epiphysis the ratio was 1.12, with the confidence interval 0.68–1.52, which leaves considerably more latitude for a possible type-2 error owing to the smaller size of the epiphyseal flow compartment.

The question of AV shunting in bone has previously been approached by Morris and Kelly (1980) and Tothill et al. (1987) in the perfused tibial nutrient artery model in normal adult dogs. They usually found nonentrapment less than 15 percent, but a few experiments preceded by ischemia were followed by up to 45 percent nonentrapment (Tothill et al. 1987). Saxena and Verdouw (1985) found no evidence of AV shunting in normal pig bone using microspheres ranging from 10–35 μm. The present study on intraosseous venous engorgement and the previous study on arthritis (Hansen et al. 1990b) were the first to study AV shunting in pathologic states. Both models pose relevant challenges to the hypothesis, because both cause precapillary vasodilation and venous stasis in juxtaarticular bone. AV shunting therefore seems unlikely as a common reaction modality in bone. We did find evidence of arteriovenous shunting somewhere in the lower extremities, because a substantial, albeit highly variable, fraction of 15-μm MSs appeared in the femoral veins. Presumably, this nonentrapment represents paw shunts, which are known to be highly temperature-sensitive (Baker et al. 1983). We found no differences between experimental and control limb with respect to nonentrapment of 15-μm MSs, but significantly more 50-μm MSs appeared in the femoral vein of the experimental limb. Perhaps, the absence of significant differences with the 15-μm MSs represents a type two error due to considerable variability. Another possible explanation is that some shunts in the 15–50-μm range, already letting 15-μm MSs pass, underwent further dilation in the experimental limb, thus allowing 50-μm MSs to escape. This interpretation is consistent with results from the joint capsule, where relatively fewer 50-μm MSs were trapped on the experimental side. Scapinelli (1968) suggested the existence of AV communications at the synovial/capsular junction in the immature knee. However, the present study provided no evidence of AV shunting in the 15–50-μm range in the control capsule, which would be a prerequisite for this interpretation.

The embolization of 50-μm MSs shifted downstream, i.e., from central to subchondral bone, relative to that of 15-μm MSs within both juxtaarticular epiphyses, which is direct evidence of intraosseous arteriolar vasodilation, as previously suggested by Bünger (1987). The trigger of this autoregulation is as yet unknown (Ewald et al. 1989, Holm et al. 1990). Obstruction of the venous drainage in skin causes arteriolar constriction by the local venoarterial reflex (Henriksen 1977), as protection against compartmental circulatory overload. This reflex has never been demonstrated in bone, and because we found arteriolar dilation during obstructed venous drainage, its existence in bone seems unlikely.

The lower relative uptake of 50-μm MSs in all the larger bony aggregates, the general underrepresentation of 50-μm MSs in arterial reference blood, and the lower concentration of 50-μm MSs in the brachial artery catheter relative to that of the aortic reference catheter confirm previous findings (Hansen et al. 1990b). The disparities must reflect uneven distribution of the two MS sizes in larger arteries due to differences in rheologic behavior.

Presumably, 50-μm MSs accumulate in the axial stream more readily than 15-μm MSs (Øfjord et al. 1981, Øfjord and Clausen 1983) and pass preferentially to the branch with the highest flow velocity at bifurcations (Yen and Fung 1978), which would be the aortic main stream at the departure point of the brachiocephalic trunk, as well as at the tip of the aortic reference catheter. The aortic sampling rate of 10 mL per min corresponds roughly to the absolute blood flow to each femur (Hansen 1990b). Because the periosteal circulation did not retain 50-μm MSs selectively, the low overall uptake of 50-μm MSs in bone must represent size-dependent microsphere skimming in arteries supplying bone.

The uneven distribution of 50-μm MSs and 15-μm MSs within bone also confirms previous results (Hansen et al. 1990b) and suggests that factors partly irrelevant to the regional flow may affect the intraorgan distribution of microspheres, such as the vascular architecture, mean arteriolar diameter, and density of major vessels. Although 15-μm MSs were evenly distributed between the brachial artery and aorta, one could suspect skimming (Yen and Fung 1978) to influence the distribution of even these small microspheres at the microcirculatory level as suggested by in vitro (Øfjord et al. 1981, Øfjord and Clausen 1983) and in vivo observations in the heart (Bassingthwaighte et al. 1988) and in bone (Hansen et al. 1990a). Comparison between deposition of microspheres and the novel plasma soluble flow marker 2-iododesmethylimipramine (the so-called molecular microsphere; Little and Bassingthwaighte 1983, Little et al. 1986) may cast light on this problem in the future.

An IAP of 75 mmHg (10KPa) impaired the femoral growth plate circulation as measured with ^{99m}Tc-diphosphonate scintimetry in immature dog knees (Hansen et al. 1989a, 1989b), which was contrary to results of the present series and previous MS studies (Bünger 1987, Holm et al. 1989, Ewald et al. 1989). However, two subtle trends in results of the present study do suggest metaphyseal impact of joint tamponade: First, 50-μm MSs entered diaphyseal cortical bone in femur more readily on the experimental side, suggesting arteriolar vasodilation in the shaft. Secondly, the experimental limb had depressed blood flow in the distal femoral metaphysis adjacent to growth plates as measured with 50-μm MSs. Thus, embolization of 50-μm MSs appeared to shift slightly away from the distal metaphyseal spongiosa, which might be viewed as a sign of precapillary vasodilation in the metaphysis acting to maintain blood flow to growth plates.

We conclude that AV shunting does not contribute to intraosseous hypertension following tamponade of the immature knee. The study provided direct evidence of intraosseous precapillary vasodilation in both juxtaarticular epiphyses of the immature knee in response to knee-joint tamponade. Finally, previous findings of different rheologic behavior of 50-μm and 15-μm MSs in the circulation were confirmed.

Acknowledgements

The study received financial support from the Danish Medical Research Council, the Danish Rheumatism Association, and the University of Århus. Technical assistance from J. Marqversen, pharmacist, and C. Flø, M.Sc., Department of Clinical Physiology and Nuclear Medicine, Århus Kommune Hospital, with all radionuclide procedures is gratefully acknowledged.

References

Arnoldi C C, Reimann I. The pathomechanism of human coxarthrosis. *Acta Orthop Scand* (Suppl 181) 1979: 1–47.

Arnoldi C C, Lemperg K, Linderholm H. Intraosseous hypertension and pain in the knee. *J Bone Joint Surg* (Br) 1975; 57(3): 360–3.

Arnoldi C C, Djurhuus J C, Heerfordt J, Karle A. Intraosseous phlebography, intraosseous pressure measurements and ^{99m}TC polyphosphate scintigraphy in patients with various painful conditions in the hip and knee. *Acta Orthop Scand* 1980; 51(1): 19–28.

Bassingthwaighte J B, King R B, Sambrook J E, van Steenwyk B. Fractal analysis of blood tissue exchange kinetics. *Adv Exp Med Biol* 1988; 222: 15–23.

Baker C H, Davis D L, Lindsey B G, Sutton E T. Temperature effects on dog hindpaw series and parallel vascular circuits. *Am J Physiol* 1983; 245(1): H159–66.

Bünger C. Hemodynamics of the juvenile knee. Joint effusion and synovial inflammation studied in dogs. *Acta Orthop Scand* (Suppl 222) 1987: 1–104.

Ewald H, Holm I E, Bülow J, Bünger C. Effect of indomethacin on regulation of juxta-articular bone blood-flow during joint tamponade. An experimental study in puppies. *Scand J Clin Lab Invest* 1989; 49(3): 273–7.

Fisher R A. *Statistical methods for research workers.* Oliver and Boyd, Edinburgh 1932.

Guba A M Jr. Arteriovenous shunting in the pig. *Plast Reconstr Surg* 1980; 65(3): 323–7.

Hansen E S, Noer I, Henriksen T B, Hjortdal V E, Bünger C. The influence of synovial effusion on juxtaarticular ^{99m}Tc diphosphonate uptake in arthritis of the immature dog knee. *J Orthop Rheumatol* 1989a; 2: 31–8.

Hansen E S, Henriksen T B, Noer I, Bünger C. Hemodynamic effects of knee joint tamponade. 99mTc diphosphonate scintimetry in growing dogs. *Acta Orthop Scand* 1989b; 60(5): 549–53.

Hansen E S, Søballe K, Kjølseth D, Henriksen T B, He S Z. Microvascular hemodynamics in experimental arthritis: Disparity between the distribution of microspheres and plasma flow in bone. *Microvasc Res* 1990a; 40: 206–17.

Hansen E S, He S Z, Hjortdal V E, Kjølseth D, Søballe K. Distribution of blood flow in normal and arthritic joints. The role of arteriovenous shunting studied with 15 µm and 50 µm sized microspheres. *Am J Physiol* 1990b. In press.

He S Z, Xiu Z H, Hansen E S, Bünger C. Microvascular morphology of bone in arthrosis. Scanning electron microscopy in rabbits. *Acta Orthop Scand* 1990; 61(3): 195–200.

Henriksen O. Local sympathetic reflex mechanism in regulation of blood flow in human subcutaneous adipose tissue. *Acta Physiol Scand* (Suppl 450) 1977.

Holm I E, Ewald H, Bülow J, Bünger C. Vasoactive substances in subchondral bone of the dog knee. *J Orthop Res* 1990; 8(2): 205–12.

Little S E, Bassingthwaighte J B. Plasma soluble marker for intraorgan regional flows. *Am J Physiol* 1983; 245(4): H707–12.

Little S E, Link J M, Krohn K A, Bassingthwaighte J B. Myocardial extraction and retention of 2-iododesmethylimipramine: a novel flow marker. *Am J Physiol* 1986; 250(6): H1060–70.

Morris M A, Kelly P J. Use of tracer microspheres to measure bone blood flow in conscious dogs. *Calcif Tissue Int* 1980; 32(1): 69–76.

Saxena P R, Verdouw P D. Tissue blood flow and localization of arteriovenous anastomoses in pigs with microspheres of four different sizes. *Pflügers Arch* 1985; 403(2): 128–35.

Scapinelli R. Studies on the vasculature of the human knee joint. *Acta Anat* (Basel) 1968; 70(3): 305–31.

Tothill P, Hooper G, Hughes S P, McCarthy I D. Bone blood flow measured with microspheres: the problem of non entrapment. *Clin Phys Physiol Meas* 1987; 8(1): 51–5.

Øfjord E S, Clausen G, Aukland K. Skimming of microspheres in vitro: implications for measurement of intrarenal blood flow. *Am J Physiol* 1981; 241(3): H342–7.

Øfjord E S, Clausen G. Intrarenal flow of microspheres and red blood cells: skimming in slit and tube models. *Am J Physiol* 1983; 245(3): H429–36.

Yen R T, Fung Y C. Effect of velocity of distribution on red cell distribution in capillary blood vessels. *Am J Physiol* 1978; 235(2): H251–7.